Received: 31 January 2025 | Accepted: 18 March 2025

DOI: 10.1002/vzj2.70019

Vadose Zone Journal

ORIGINAL ARTICLE

Using relative gas diffusivity to highlight soil compaction issues with possible effects on N efficiency in grain corn production, southern Quebec, Canada

Jean Caron[1] | **Vincent Grégoire**[1] | **Alain N. Rousseau**[2] | **Jacynthe Dessureault Rompre**[1] | **Gabriel Deslauriers**[3] | **Diane Bulot**[1] | **Josselin Bontemps**[1] | **Didier Vieux**[1] | **Thiago Gumiere**[1] | **Hossein Bonakdari**[4]

[1]Département des sciences du sol et de génie agroalimentaire, Université Laval, Quebec, Canada

[2]INRS-ETE, Quebec, Canada

[3]Groupe Pleine Terre, Napierville, Quebec, Canada

[4]Department of Civil Engineering, University of Ottawa, Ottawa, Ontario, Canada

Correspondence
Jean Caron, Département des sciences du sol et de génie agroalimentaire, Université Laval, Quebec, Canada.
Email: jean.caron@fsaa.ulaval.ca

Assigned to Associate Editor Muhammad Naveed.

Funding information
Natural Sciences and Engineering Research Council of Canada; Axelys; Réseau québécois de recherche en agriculture durable (RQRAD); Elmec Inc.; Soleno Inc.; Groupe Pleine Terre

Abstract

It has long been suggested that soil compaction indices should be monitored as part of a routine soil management program. Moreover, in addition to properties related to storage of gases and fluid within a bulk volume (i.e., bulk density [BD] and air porosity [θ_a]), some authors have suggested that properties linked to fluid and gas exchanges such as gas diffusion and hydraulic conductivity should be used to assess the physical health of soils. Given the risk of severe compaction due to the increasing size of farm equipment and the lack of long rotation in cash crop production, data on soil storage and exchange properties need to be collected. The objective of this study was to assess the physical soil health of the top 30 cm of 18 southern Quebec corn fields using a set of indicators. The data were also used to determine crop response to nitrogen fertilization. The results showed that over 93% of the corn fields had a relative gas diffusivity (D_s/D_o) below the 0.03 threshold at both 15- and 30-cm depth, suggesting substantial crop growth limitations. They also showed that around 40% of the soils had subsurface drainage problems linked to a low saturated hydraulic conductivity (49% at 15 cm and 47% at 30 cm lower than 0.001 cm s^{-1}). The levels of relative gas diffusivity were low, not only limiting crop growth but also likely reducing nitrogen efficiency through increasing risk of denitrification. Moreover, the results suggest that in some fields, high yields can be achieved with as little as 60 and up to 215 kg of nitrogen per hectare, and that slow-draining soils will have a very poor response to N fertilization, leading to lower net revenues and nitrogen losses. Overall, the findings suggest that appropriate soil conservation and water management practices based on soil physical health criteria like relative gas

Abbreviations: ACE, autoclaved-citrate extractable; BD, bulk density; BG, β-glucosidase; CHU, corn heat units; FDA, fluorescein diacetate hydrolysis; LIME, local Interpretable Model-Agnostic Explanations; MERN, most economic rate for nitrogen; MR, microbial respiration; MUB, methylumbelliferone; P-E N, post-emergence nitrogen; P-E NO_3–N, post-emergence NO_3–N; PVC, polyvinyl chloride; SOM, soil organic matter.

diffusivity and hydraulic conductivity must be implemented to maintain or improve soil productivity and health in the face of climate change.

Plain Language Summary

Intensive corn and soybean production may increase the risk of compaction due to loss of organic matter, residues, and continuous action of deep rooting systems. A survey study conducted in southern Quebec in soil under continuous corn production showed that soils that had been cropped continuously for many years are now dense enough to show severe lack of air and poor drainage, hence restricting root development and increasing the risk of losing beneficial effect of mineral fertilizers like nitrogen on crop development. This study also identified potentially useful highly sensitive indicators linked to aeration and drainage processes.

1 | INTRODUCTION

For more than 50 years, soil compaction has been a concern and is the result of increasing load per tire (Batey, 2009), increasing farm equipment weight (Batey, 2009; Keller & Or, 2022), lack of deep rooting soil rotations, and loss of soil organic matter (SOM; Ball, 2013). Over the last two decades, detrimental pressure on soil health has increased with an increasing overall global demand for cash crops because of a growing world population, an increasing demand for corn and soybean for livestock production, and increased production costs. Moreover, farms have been continuously increasing in size with less farmers all over the world (Mehrabi, 2023). Conversion to cash crops has resulted in less pasture and less use of forage in cash crop rotations, with expected degradation of critical physical properties linked to aeration and drainage (Reynolds et al., 2014). Indeed, bringing forages into rotations is well known to improve aeration and drainage due to the modification of air-filled porosity (θ_a) and saturated hydraulic conductivity (K_s; Reynolds et al., 2014; Meek et al., 1990; Caron et al., 1996). Also, forages bring additional benefits relative to continuous corn production, linked to deep rooting and organic matter deposition (Angers & Caron, 1998; Meek et al., 1990; Reynolds et al., 2014). Finally, the gradual move from dairy and cattle farming to monoculture has resulted in less and less manure applications. All these changes in production systems have led to a gradual loss of organic matter, with subsequent deleterious effects on critical soil physical properties among others.

Along with the increasing weight of farm equipment, soil compaction is moving increasingly into deeper zones within the profile, well below the plow layer down to 50 cm and deeper (Batey, 2009; Håkansson et al., 1987; Keller & Or, 2022). Compaction to deeper horizons becomes critical as it might be difficult to detect and mitigate as plowing, subsoiling, and annual freezing give inconsistent results and, thus, it is expected to last over many crop cycles (Batey, 2009; Gameda et al., 1987, Håkansson et al., 1987). It will have an obvious effect on root system development, restricting aeration and exploration of the upper part of the soil profile adversely affecting crop yields (Stepniewski et al., 1994). Moreover, as compaction is associated with loss of pore continuity in most studies (Xu et al., 1992), deep compaction will seriously impact the drainage capacity of soils, with possible negative effects on infiltration (Caron et al., 1996; Meek et al., 1990), drainage, and runoff (Batey, 2009) even if sometimes it may have positive effects on dry years (Yi et al., 2022). Denitrification is also expected to increase with poor drainage conditions (Balaine et al., 2013; Ball, 2013; Batey, 2009).

Soil compaction has received early, yet surprisingly limited attention since then, possibly linked to the lack of resources and difficulty in implementing large-scale assessments. A recent (January 2024) consulting of publications accessed through Web of Science indicated a 10-fold larger number of published papers on soil management than on soil compaction over the 1900–2020 period, although it is common knowledge that such assessments should be included in any soil management program (Batey, 2009).

When assessments/measurements are performed, the tools used in most studies have a limited sensitivity. Indeed, it has long been suggested by numerous authors (Balaine 2012; Balaine et al. 2013, 2016; Ben-Noah & Friedmann 2018; Nkongolo et al., 2010; Stepniewski et al., 1994) that soil properties such as gas diffusion control key processes linked to respiration and greenhouse gas emissions. With respect to drainage of the top layer, K_s is a good indicator of pore continuity critical to water movement (Ball et al., 1988). Such soil characteristics linked to exchange of fluids and gases are referred herein as dynamic properties in opposition to those

linked to the storage of fluid and gases within the bulk soil and referred herein as static properties (bulk density and air-filled porosity), even if these properties may vary in time at a specific field location. Therefore, in addition to static properties (bulk density [BD] and θ_a) and penetrometer resistance, gas diffusion and K_s should be measured to monitor the physical health of soils. Additionally, these latter two dynamic indicators have been linked to greenhouse gas emissions (Balaine et al., 2013, 2016; Chamindu et al., 2019; Nkongolo et al., 2010) and productivity and environmental outcomes (Hu et al., 2021).

In the growing media manufacturing industries, the advantages of dynamic over static indices to assess crop productivity have long been established in numerous publications (Allaire et al., 1996; Boudreault et al., 2014; Caron, 2004; Caron et al., 2005, 2013, 2015). Hence, both dynamic and static indicators are among the recommended parameters for the manufacturing and quality control of growing media (Caron et al., 2022). However, for cultivated agricultural mineral soils, most field studies on mineral soils have focused on static indicators only, as again revealed from the number of publications. Indeed, out of the 1400 papers listed on soil compaction, less than 30 linked soil compaction with gas diffusivity (Web of Science consulted January 2024). Difficulty, affordability, and ease of measurements have often been key arguments for limiting the use of dynamic indices. Fortunately, the development of in situ technique and sensing technologies now provides easier and faster means of measuring in situ dynamic properties like relative gas diffusivity (D_s/D_o), soil respiration rate and K_s, and thus should help increase their use at field scale.

Studies on soil health are often limited to the top 0–30 cm of the soil profile despite a recognized risk of deeper compaction due to increasing farm equipment weight (Batey, 2009). Therefore, there is an increasing need to investigate the extent of compaction and use dynamic indices that might be more sensitive for detecting compaction problems at different depths of the profile. This study was built around three objectives. The first one assessed the extent of compaction of the top 30 cm of soils supporting the most popular cash crops in southern Quebec, Canada, that is corn and soybean. This area grows 81% of the grain corn cultivated in Quebec (https://www.quebec.ca/agriculture-environnement-et-ressources-naturelles/agriculture/industrie-agricole-au-quebec/productions-agricoles/culture-grains-cereales-oleagineux). The second objective compared the representativity of static (BD, θ_a) and dynamic (K_s and D_s/D_o) parameters as key soil health indicators, and their relationships with crop productivity. Finally, the third objective evaluated the potential effects of different compaction levels on the corn response to nitrogen fertilization for different soil conditions.

Core ideas

- About 90% of corn fields had a relative gas diffusivity below the 0.03 threshold, suggesting crop growth limitations.
- The levels of relative gas diffusivity were low enough for increasing the risk of denitrification.
- Soil relative gas diffusivity and hydraulic conductivity are highly relevant soil health indicators.
- About 40% of the soils had potential subsurface drainage problems.

2 | MATERIALS AND METHODS

2.1 | Soil formation in the surveyed area

The soil parent materials partially follow the underlying geology, varying from the metamorphic rocks in the Appalachian region to softer sedimentary rocks underlying the St. Lawrence valley and the sediments laid down since the emergence of Quebec from the last glaciation. Indeed, with the ice sheet retreating northwards, the land surface became covered with a thin layer of sandy/stony till. Thus, Quebec soils have formed over the last 6000–10,000 years, during which the climate has warmed, and vegetation has moved northwards to occupy the glacial sediments. The current climate in southern Quebec has a mean annual temperature of 7°C around Montreal (45°N) and annual precipitation ranges of about 1000 mm in the south with 80%–90% of precipitation falling as rain with the remaining in snow (Moore, 2021).

2.2 | Experimental sites

This study is based on a random sampling of 18 different sites over 3 years from a large N fertility replicated trial plots in southwestern Quebec. Soil texture had clay contents varying from 5% to 61% and organic matter from 1.4% to 5.9% (w/w) as shown in Table 1. At the initial stage of this study, in 2019, sampling was preferentially performed on three sites with an experimental setup suspected to have compacted zones, according to field agronomists, and based on previous soil pith observations and BD measurements at different locations within these sites. Given preliminary results of 2019, sampling was then extended to 11 and four additional sites in 2021 and 2022, randomly selected among a total of 30 sites of replicated plots maintained through the four years for N fertility trials. Hence, a total of 18 sites were sampled over the 3-year study. For each site, a corn fertility trial was performed, in a

TABLE 1 Textural and soil organic matter content of the different sites sampled in this study.

Site	Year	Sand, % (w/w)	Silt, % (w/w)	Clay, % (w/w)	SOM, % (w/w)	Textural class
1	2019	61	28	11	2.5	Sandy loam
2	2019	55	28	17	2.5	Sandy loam
3	2019	35	43	22	4.7	Loam
4	2021	0	45	55	5.9	Silty clay
5	2021	1	58	40	3.9	Silty clay
6	2021	33	47	20	3.3	Loam
7	2021	0	39	61	4.9	Clay
8	2021	0	56	44	4.8	Silty clay
9	2021	0	65	35	2.8	Silty clay loam
10	2021	46	37	17	1.4	Loam
11	2021	7	46	47	3.1	Silty clay
12	2021	0	52	48	4.2	Silty clay
13	2021	0	42	58	5.8	Silty clay
14	2021	4	57	38	2.8	Silty clay loam
15	2022	10	72	19	3.2	Silt loam
16	2022	61	34	5	3.0	Sandy loam
17	2022	29	34	38	2.4	Clay loam
18	2022	30	56	14	3.2	Silt loam

complete block randomized design with three replicates. On each site, five or six rates of N were randomly allocated (0–50–100–150–200–250 kg N ha^{-1}) and applied after seeding (V4–V6 growth stages) to different experimental units. This was applied on top of a 50 kg N ha^{-1} as a starter every year of the trials. Each experimental unit was constituted of four rows spaced × 76 cm (3.04-m wide), side by side with the neighboring block, and 10-m long.

2.3 | Soil sampling

Sampling took place during the growing season from July to October prior to harvest. Aluminum cores (8 cm in diameter × 5.5-cm long) were inserted into a sharpened 1-cm long sampling ring and driven into the soil with a hammer over three different soil layers (depths of 12.5–17.5 cm and 27.5–32.5 cm) for a total of 15 cores per layer per site. Such a core size was chosen as large as possible to provide a representative elementary volume for adequate relative gas diffusivity and total porosity measurements (Piccoli et al., 2019), but at the same time, small enough to be hammered with minimal effort and disturbance by trained field operators in compacted horizons. The volume reached (276.5 cm^3 cm^{-3}) was in between the intermediate (100.4 cm^3 cm^{-3}) and the largest one (628.3 cm^3 cm^{-3}) studied by Piccoli et al. (2019). Once at the proper depth (12.5 or 27.5 cm for the 15- and 30-cm sampling depth), a shovel was pushed below the core and handled to remove the cores. Then, a large knife was used to detach any adhering soil. The bottom and top-soil surface within the ring was leveled up by using a sharpened knife. A custom lid and a rubber band were used to cover the top and bottom surface. For chemical and biological analysis, soil samples were taken with an auger to a depth of 0–20 cm. Samples were transported within a rigid plastic cooler and later stored at 4°C prior to analysis prior to sieving or analyses on cores.

2.4 | Soil preparation

The sample preparation protocol for the analyses carried included sieving the fresh samples to 2 mm followed by the preparation of five subsamples for the different analyses. Two of the subsamples were frozen at −20°C to carry out analyses of enzymatic activity and total microbiological activity (see below). A subsample was dried at 65°C for microbial respiration analysis. Another subsample was air dried for additional analysis.

2.5 | Measurements of physical properties

Static and dynamic analyses of soil physical parameters were performed within 2 months after sampling and storage in a fridge at 4°C. Once removed from the fridge, soil cores were fitted with a 15-cm extension and saturated with water from bottom up for 24 h at room temperature prior to being used for K_s measurements.

The constant-head soil core method was used, a method where water is flowing through the soil core at a steady rate under a constant hydraulic head gradient (Reynolds, 2008). The water flow was deduced from pressure changes within a Mariotte reservoir equipped with a pressure sensor linked to a data acquisition system, allowing to fit for K_s value (Reynolds, 2008).

After completion of K_s measurements, cores were transferred onto a tension table to derive the water desorption curve (0- to 10-kPa range, with equilibrium at −0.27, −1, −3, −5, and −10 kPa cm of soil water potential (Reynolds & Topp, 2008). At equilibrium, samples were removed and weighed to determine the gravimetric water content later converted to volumetric water content (θ) using BD. Soil subsidence in the cores was also repeatedly measured at all potentials but was found to be limited to 1 or 2 mm at the most, when occasionally occurring since they were non-swelling soils and compacted samples. Once completed, samples were dried at 105°C up to equilibrium. Weighing the samples in the cores allowed BD determination using the soil core volume. The water desorption curve was then modeled using the van Genuchten's model (van, Genuchten,1980) as follows:

$$\Theta = \left(\frac{1}{1+(\alpha h)^n}\right)^m, \tag{1}$$

where Θ is the normalized water content; $\Theta = \frac{\theta-\theta_r}{\theta_s-\theta_r}$, where subscripts s and r indicate the saturated and residual values for volumetric water content θ ($cm^3\ cm^{-3}$), h is the soil water potential (kPa), while α, n, and m are parameters. Four out of five parameters (θ_r, α, n, m) were fitted independently by minimizing the sum of square errors on the six experimental points. The fifth parameter, θ_s, was fixed and imposed to the maximum volumetric water content measured.

Fitting of the water desorption curve (fitting α, n, and m and imposing the measured θ_s) was performed using the R programming language with the "optim" function of the "stats" package (R Core Team, 2023). The "L-BFGS-B" method was employed with a user-defined function evaluating the mean square error of modeled versus observed water contents.

Air-filled porosity (θ_a) was evaluated by using two points of the fitted retention curve: water content at saturation and that at −5 kPa (corresponding to around 51 cm of soil matric potential, and then by subtracting the latter from the former). This is obviously wetter than field capacity, as field capacity is expected to be more in the range of −10 kPa according to many authors for soils in the area (Gasser et al., 2023). However, given that the purpose of the present study was to try to link aeration properties likely to occur early in the spring, this potential was chosen as it better corresponded to the early drainage phase soil water potential prevailing at the 0- to 30-cm depth in the early spring, based on common field observations (see results section on water table Figure 3).

Relative gas diffusivity (D_s/D_o), the ratio of the gas diffusivity to that in free air at the same temperature, was calculated using the following relationship:

$$\frac{D_s}{D_o} = \frac{\theta_a}{\tau}, \tag{2}$$

where τ is for pore continuity (Caron & Nkongolo, 2004), defined as (Equation 3):

$$\tau = \frac{0.00028\rho g}{\eta K_s}\int_{\theta_{lg}}^{\theta_{ea}} \alpha^2\left(\Theta^{-\frac{1}{m}}-1\right)^{-2/n} d\theta, \tag{3}$$

where η is water viscosity (Pa s), ρ is water density (g cm^{-3}), and g is gravitational acceleration (m s^{-2}). The water content used for the lower integration limit for relative gas diffusivity calculations in Equation (3), θ_{lg}, was set to −5 kPa as pores associated with lower soil water potential have a negligible influence for calculating D_s/D_o (Caron & Nkongolo, 2004). The upper integration limit, θ_{ea}, which represents the water content at the point of air-entry, was calculated using the water desorption curve, where the potential at which water content dropped by 0.01 $cm^3\ cm^{-3}$ from total porosity (Nemati et al., 2002).

2.6 | Soil chemical and biological analyses

Soil chemical analysis included Mehlich-3 extractable elements (P, K, Ca, Mg, Al), nitrates, enzymes activity for N-acetyl-β-D-glucosaminidase (NAG) and β-glucosidase (BG), potential total microbial activity as measured with fluorescein diacetate hydrolysis (FDA), microbial respiration (MR), and autoclaved-citrate extractable (ACE) soil proteins.

The Mehlich-3 method (CEAEQ, 2014; Ziadi & Tran, 2008) involved scooping 3 cm^3 of air-dried soil sieved to 2 mm and adding 30 mL of M-3 extraction solution consisting of 0.2 M CH_3COOH, 0.25 M NH_4NO_3, 0.015 M NH_4F, 0.013 M HNO_3, and 0.001 M EDTA to achieve a soil:solution ratio of 1:10. After 5 min of agitation at 120 rpm, the mixture was filtered through a Whatman #42 filter paper. The quantification was performed using inductively coupled plasma mass spectrometry (ICP-MS).

Nitrates were quantified according to the AZ-5 method of the CPVQ (1993), weighing 5 g of air-dried soil sieved to 2 mm and adding 25 mL of a 2 M KCl extraction solution, followed by filtering after 30 min of agitation at 120 rpm. The filtrate was analyzed using a Technicon A.A. II autoanalyzer.

Enzymatic activity indicators, NAG and BG, were measured following the protocol of Bell et al. (2013). Briefly, two

suspensions of 1.2 g of fresh (thawed) soil in 40 mL of 50 mM sodium acetate solution were stirred at 350 rpm for 60 s. Then, 1 mL of the suspension was pipetted into a microcentrifuge tube. Six standards of 4-methylumbelliferone (MUB) were prepared at the following concentrations: 0, 2.5, 5, 10, 25, and 50 µM. The microtubes were then incubated for 1.5 h at 25°C and centrifuged at 13,000 rpm for 1 min before being transferred into a 96-well opaque microplate, with 50 µL of each MUB standard and 200 µL of soil suspension for the standard curve, and 250 µL per well for each of the two enzymes. The plate was then read for fluorescence with a spectrophotometer set to an emission of 450 nm and an excitation of 365 nm.

Total microbial activity was assessed using the FDA analysis according to the protocol established by Adam and Duncan (2001), which involved measuring absorbance at 490 nm with a spectrophotometer. A suspension of 1.2 g of fresh soil in 9 mL of 60 mM potassium phosphate buffer was mixed with a solution of fluorescein diacetate (3′6′ diacetyl-fluorescein) at 1000 µg mL^{-1}. Two tubes contained the FDA solution, and one tube without the FDA solution served as a control. After 20 min of agitation at 100 rpm and 28°C, 2 mL of the supernatant was transferred into microcentrifuge tubes for centrifugation at 7800× g for 2 min. Finally, 300 µL of the supernatant from the tubes was transferred into the wells of a 96-well microplate for absorbance reading at 490 nm.

ACE soil proteins were quantified following the protocol of Hurisso et al. (2018). After weighing 1.25 g of air-dried soil, 10 mL of 0.02 M sodium citrate solution was added and shook at 180 rpm for 5 min, autoclaved for 30 min at 121°C, and then clarified by centrifugation at 10,000 g for 3 min. A 50:1 solution of reagents A and B was prepared (BCA solution). Eight standards of bovine serum albumin (0, 125, 250, 500, 750, 1000, 1500, and 2000 µg mL^{-1}) were used for the standard curve using 10 µL of each standard. Two replicates of each sample (10 µL) were added to the microplate. Finally, 200 µL of the BCA solution was added to all wells of the microplate. The reaction involved incubating the microplate for 60 min at 61.5°C and then reading the absorbance at 562 nm with a spectrophotometer.

Microbial respiration was measured using an EGM-5 infrared gas analyzer (PP Systems), adapted from the method of Haney et al. (2008). Soil samples sieved to 2 mm were dried at 65°C for 24 h. Subsequently, 2.5 g of soil was rehydrated to 50% of water pore filled space, following the Haney et al. (2008) protocol, using distilled water in a 10-mL vial (Agilent, 10 mL, 5182-0838). The amount of water added was calculated based on the bulk density of the dried soil once adjusted for organic matter content for determining the total porosity of the sample. The vial was then placed in a 250-mL Mason jar whose lid was pierced and then hermetically sealed with a septum (Wheaton cat. 224 100202, Millville, NJ, USA). The setup was left to be incubated 24 h, after which the release of CO_2 was measured. Jars without soil were used as blank measurements.

2.7 | Piezometer data

In 2021, five equally spaced piezometers were installed in five randomly chosen sites being also sampled for yield and soil health indicators on the same year. Standpipes were positioned perpendicular to the subsurface drains direction and properly spaced to cover the expected spacing between two adjacent parallel drains. Standpipe, made of 2-inch diameter polyvinyl chloride tubing with a 4-inch strained bottom, were inserted down to 1 m after augering an insertion hole. Then, a HOBO U20L Water Level Logger (Model U20L-04; Hobo) was inserted into the pipe and maintained at a fixed depth using a small rope knotted to the upper piezometer part. Surface soil was densely packed around the pipe at the 30- to 40-cm depth to avoid preferential flow. The sensors were used to monitor water level and temperature through fall 2021 (after plowing) up to the following spring (2022), prior to secondary tillage.

2.8 | Corn yields and the most economic rate for nitrogen for corn

For corn dry yields, cobs were collected on 4-m long (2 m on each side of the plot center) of each of the two central rows within each replicate. Cobs were then threshed, grains weighed, and water content was determined after drying at 60°C for 3 days prior to determining the total dry weight of the cobs and their specific weight. Grain dry yields were then converted to kilograms per hectare using the surface of the experimental unit and the final plant density. The most economic rate for nitrogen (MERN) was calculated by using the following formula (Rosser, 2022).

$$\mathrm{MERN} = \frac{\text{Price ratio } (\$\ \mathrm{kg}\ -\ \mathrm{N}\ :\ \$\mathrm{kg}\ -\ \mathrm{corn}) - b}{2 \times a}, \tag{4}$$

where a and b are the quadratic, and the linear coefficient of the quadratic nitrogen (N) yield response (Y) curve (Equation 5) fitted to each individual site (see below).

$$Y = a\mathrm{N}^2 + b\mathrm{N} + c. \tag{5}$$

A price ratio of 7.44 (kg of N per kg of corn) was chosen based on the average price for corn from September 2023 to September 2024 in Quebec as well as an average price for nitrogen (UAN 28-0-0) at 500$ Canadian dollars per metric ton.

2.9 | Statistics and aggregated data

For the classical statistical analysis or for using artificial intelligence (see below), site-specific weather indicators were added to consider temperature and precipitation. The nearest available public weather station was used for each site (Audet et al., 2012). The average distance between a site and a public station was 10 km, and the maximum was 17 km. Monthly cumulative rainfall over the growing season was added to the data set and based on daily values. Corn heat units (CHU) were also calculated monthly according to local guidelines (Bourgeois et al., 2012; Lepage & Bélanger, 2012). Basic statistics and conventional and stepwise regressions were performed using SAS 9.4 (SAS Institute).

2.10 | Statistical and artificial intelligence analysis

For a clear understanding of the acting mechanisms, multiple regression is helpful to test the significance and the relative contribution of the different variables and was therefore used herein for relative quantification of the different variables. However, given the fact that it does require data to conform to specific statistical assumptions, that complex unknown effects and collinearity may affect models built with classical multiple regression, artificial intelligence analysis was also performed as a comparative tool to strengthen the conclusions.

With both approaches, the following variables were included: corn dry yield, total porosity taken equal to saturated volumetric water content θ_s, air-filled porosity θ_a at −5 kPa saturated hydraulic conductivity K_s (its log10 value), relative gas diffusivity D_s/D_o (its log10 value), rainfall and CHU from May to October, pH and buffer pH, organic matter SOM, Mehlich-3 extractable elements (P, K, Ca, Mg, Al), nitrates, enzyme activity indicators (NAG and BG), potential total microbial activity (FDA), microbial respiration, and ACE soil proteins.

Out of 248 rows in the data set, 47 had one or more missing data, due to numerous factors (parameters not measured because of time or financial constraints, D_s/D_o not estimable, missing yield within a replicate, etc.). This resulted in a total of 201 samples for training and testing purposes. For the machine learning model, 145 samples were randomly selected for training, with the remaining 56 rows used for testing. This was done using a random selection without a replacement approach to create thorough training and testing data sets. In the first attempt, all 38 input variables (features) were utilized to forecast the target variable. The input features were standardized through the min-max scaling method to align the inputs and improve the accuracy of the model.

To measure feature importance, the Local Interpretable Model-Agnostic Explanations (LIME) technique was utilized in the machine learning approach. The coefficients of the linear model generated by LIME indicated the strength and direction of the relationship between each feature and the prediction. A positive coefficient means that an increase in the feature's value is associated with an increase in the predicted outcome, while a negative coefficient signifies that an increase in the feature's value is associated with a decrease in the predicted outcome. Features were ranked based on the absolute value of these coefficients; a larger absolute value corresponded to a higher rank and greater influence on the model's prediction. Instead of using all 38 important variables, the LIME results helped in selecting the top 10 features to develop a new machine learning model. The model's accuracy was slightly better than the one using all inputs.

3 | RESULTS AND DISCUSSION

Table 2 summarizes the whole data set obtained over 3 years for physical, chemical, and biological indices. On average, considering all plots and applied nitrogen, yield is 11,412 kg ha^{-1} with an average of 100 kg + 50 kg starter applied, a pH of 6.3, 3.8% organic matter, 508 mm precipitation from May to October, and 3427 corn heat units during the same period.

Figure 1a,b presents two static indicators for the sample sites over the 3 years, that is, bulk density and air-filled porosity. In the top 15 cm, most of the bulk densities are lower than 1.5 g cm^{-3} (1.46 g cm^{-3}), but at the depth of 30 cm, about 50% of them have densities greater than this value (mean of 1.51 g cm^{-3}). A bulk density of 1.5 g cm^{-3} has been identified as the threshold above which crop growth may be severely impacted, particularly in clay soils (Daddow & Warrington, 1983). Such level may not be critical if drainage and air exchange are adequate and if the air-filled porosity is still high. However, the air-filled porosity data indicated important aeration limitations in the first 30 cm of soils, as 87% of the samples were below the 10% level (mean of 0.056 cm^3 cm^{-3}), a level associated with soils with aeration limitations (Gliński & Stępniewski, 2018).

Aeration of the top 15 cm was slightly better, but on average, the value reached 0.061 cm^3 cm^{-3}, which is still a characteristic of aeration limitations. These results corroborate data from Gasser et al. (2023) who sampled and analyzed 426 cultivated sites over 5 years and came to very similar conclusions for the same soil series. Similar losses of aeration of cultivated sites were already reported by Tabi et al. (1990) in the same area and therefore do not seem to have improved with time.

Consistent with static indicators, Figure 1c,d shows values of dynamic indicators (K_s and D_s/D_o) of cultivated sites. It

TABLE 2 Variable used in this study with their means and basic statistics for all sites and all years in this study.

Variable	Abbreviation	Units	Mean	Geometric mean[a]	Minimum	Maximum	Standard deviation
Year	Year				2019	2022	
Plot number	Plot		203		101	306	80.9
Yield	Yield	kg ha^{-1}	11411.9		4057	17277	2311
Post-emergence nitrogen	P-E N	kg ha^{-1}	100		0	250	71.7
Soil pH	pH		6.3		5.5	7.5	0.49
Buffer pH	Buffer pH		6.8		6.3	7.9	0,39
Soil organic matter content	SOM	g g^{-1}	3.80		1.54	6.23	1.28
Mehlich P	P	kg ha^{-1}	135.3		58.2	228.3	54.8
Mehlich K	K	kg ha^{-1}	467		140	735	176
Mehlich Ca	Ca	kg ha^{-1}	7499		2595	12105	2616
Mehlich Mg	Mg	kg ha^{-1}	937		172	1595	452
Mehlich Al	Al	ppm	1026		738	1211	154
Post-emergence NO_3–N	P-E NO_3–N	mg kg^{-1}	18.7		7.8	54.2	9.6
Harvest NO_3–N	Harv. NO_3–N	ppm	33.4		2.9	255.0	38.2
BG enzyme activity	BG	nmol g^{-1} h^{-1}	15.5		0.4	102.7	17.4
NAG enzyme activity	NAG	nmol g^{-1} h^{-1}	26.4		1.9	64.1	15.0
Potential total microbial activity by FDA	FDA	μh g^{-1} kg^{-1}	10670		0	43387	7768
Microbial respiration	MR	mg C-CO_2 kg^{-1} h^{-1}	3.29		0.04	8.02	1.02
Autoclaved-citrate extractable soil proteins	ACE	g kg^{-1}	3.61		1.04	8.11	1.34
Bulk density at 15 cm	BD 15cm	g cm^{-3}	1.46		1.04	1.83	0.14
Bulk density at 30 cm	BD 30cm	g cm^{-3}	1.518		1.163	1.892	0.132
Soil saturated water content at 15 cm	θ_s 15cm	cm^3 cm^{-3}	0.445		0.320	0.578	0.048
Soil saturated water content at 30 cm	θ_s 30cm	cm^3 cm^{-3}	0.435		0.297	0.548	0.050
Soil air porosity at 15 cm	θ_a 15cm	cm^3 cm^{-3}	0.061		0.012	0.253	0.037
Soil air porosity at 30 cm	θ_a 30cm	cm^3 cm^{-3}	0.056		0.010	0.237	0.039

(Continues)

TABLE 2 (Continued)

Variable	Abbreviation	Units	Mean	Geometric mean[a]	Minimum	Maximum	Standard deviation
Hydraulic conductivity at 15 cm	K_s 15cm	cm s^{-1}		2.4E-03	9.18E-07	6.93E-01	
Hydraulic conductivity at 30 cm	K_s 30cm	cm s^{-1}		1.4E-03	3.66E-07	3.28E-01	
Relative gas diffusivity at 15 cm	D_s/D_o 15cm	cm^2 s^{-1} cm^{-2} s^1		8.6E-04	1.38E-07	3.71E-01	
Relative gas diffusivity at 30 cm	D_s/D_o 30cm	cm^2 s^{-1} cm^{-2} s^1		5.5E-04	1.68E-08	1.93E-01	
Rainfall of May	Rain May	mm	26.7		2.3	87.1	32.2
Rainfall of June	Rain June	mm	97.0		56.0	181.1	42.4
Rainfall of July	Rain July	mm	84.1		56.7	117.2	17.2
Rainfall of August	Rain Aug.	mm	81.4		45.2	170.3	41.8
Rainfall of September	Rain Sept.	mm	91.9		71.0	136.7	20.8
Rainfall of October	Rain Oct.	mm	127.3		0.0	249.1	63.3
Corn heat unit of May	CHU May	˚C	321		178	432	72
Corn heat unit of June	CHU June	˚C	704		602	761	52
Corn heat unit of July	CHU July	˚C	760		710	850	45
Corn heat unit of August	CHU Aug.	˚C	796		699	865	40
Corn heat unit of September	CHU Sept.	˚C	549		462	607	38
Corn heat unit of October	CHU Oct.	˚C	296		19	359	91

Note: Corn units and rainfall were cumulated for each month separately, from May to October and for the same year.

[a]Geometric means are provided for log10-transformed variables

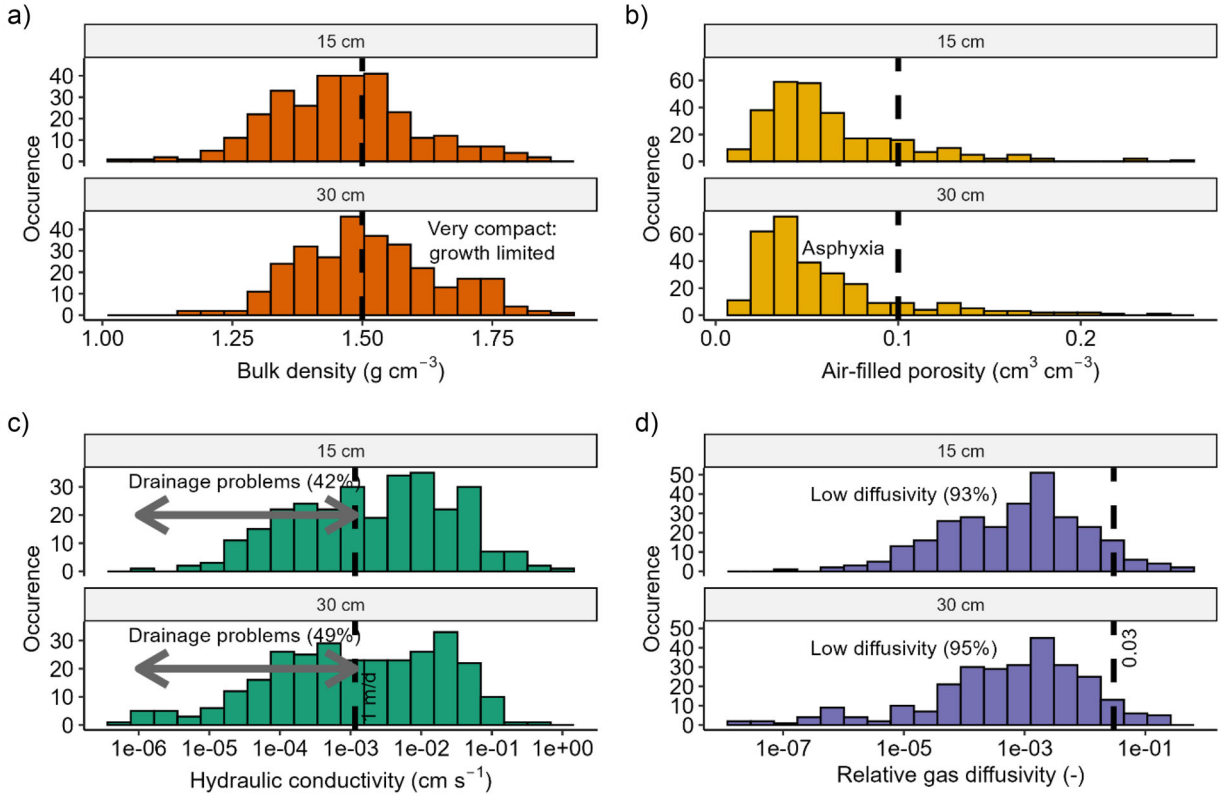

FIGURE 1 Values of static and dynamic indicators for depths for the whole 3-year data sets at the 15-cm and 30-cm depth: (a) bulk density, (b) air-filled porosity at −5 kPa, (c) saturated hydraulic conductivity, and (d) relative gas diffusivity at −5 kPa.

also pointed out important signs of physical property degradation, reaching sub-optimal conditions. For K_s, 42% at 15 cm and 49% at 30 cm of K_s values were below 1 m per day, a value characterizing soils having drainage problems which are known to increasingly affect crop productivity in these humid production environments (Chabot et al., 2022; Reynolds et al., 2014; Thériault et al., 2019). Relative gas diffusivities were also below the critical limit of 0.026–0.038, that is, ≈0.03, identified by Balaine et al. (2016) and Chamindu et al. (2019) as the upper threshold of N losses via the denitrification for incubated soil cores. In our study, between 93% (15-cm depth) and 95% (30-cm depth) of the values were below a D_s/D_o value of 0.030. Below this threshold for the whole 0–40 cm, it can be shown with steady-state models (Glinski & Stepniewski, 2018) that oxygen deficiency will occur in the first 40 cm of soil at field capacity within a day or so, with a respiration rate of 10^{-6} g O_2 cm^{-3} s^{-1}. Also, it has been reported by Balaine et al. (2013, 2016) and Chamindu et al. (2019) that denitrification will increasingly become important as soil microbes will start accepting electrons from nitrate, iron, sulfur, and carbon when facing decreasing oxygen levels. Therefore, all studied indicators consistently point toward obvious signs of land degradation associated with long-term cash crop production at levels potentially affecting crop productivity and efficient nitrogen use.

3.1 | Comparing performances of key soil health indicators and their relationship with crop productivity

The relevance of static (bulk density, air filled porosity) and dynamic (saturated hydraulic conductivity and relative gas diffusivity) indicators were compared to assess the need of measuring them on a routine basis.

3.1.1 | Classic correlation

When using the yields of the whole data set (see Table 3), significant positive correlations were found between yields and applied nitrogen ($r = 0.47$, $p < 0.0001$), the logarithm (base 10) of relative gas diffusivity D_s/D_o at 15 cm ($r = 0.41$, $p < 0.0001$) and at 30 cm ($r = 0.23$, $p < 0.0001$) and saturated hydraulic conductivity K_s at 15 cm ($r = 0.16$, $p < 0.008$) and surprisingly, bulk density BD at depths of 15 cm ($r = 0.13$, $p < 0.03$) and 30 cm ($r = 0.20$ $p < 0.0007$). Negative correlations were observed between air-filled porosity and crop yield ($r = -0.32$, $p < 0.0001$) at 15 cm and at 30 cm ($r = -0.20$, $p < 0.0009$). This is quite surprising to see a positive correlation between BD and crop yields given the relatively high value (1.5 g cm^{-3}) of the samples. The significant negative

TABLE 3 Correlation matrix between soil physical properties (static and dynamic) and corn dry yields for the 3-year data set 15 and 30 cm (N = 282–290 observations).

	Post emergence applied N	BD 15 cm	BD 30 cm	θ_s 15 cm	θ_s 30 cm	θ_a 15 cm	θ_a 30 cm	D_s/D_o 15 cm	D_s/D_o 30 cm	K_s 15 cm	K_s 30 cm
Corn dry yield	0.47	0.13	0.20	−0.08	−0.11	−0.32	−0.19	0.41	0.23	0.16	0.11
	<0.0001	**0.0252**	**0.0007**	0.1565	0.0679	**<0.0001**	**0.0009**	**<0.0001**	**<0.0001**	**0.0082**	0.062
BD 30 cm	0.11	0.54	1.00	−0.55	−0.88	0.04	−0.26	−0.02	0.05	−0.06	−0.12
	0.0553	**<0.0001**		**<0.0001**	**<0.0001**	0.5536	**<0.0001**	0.7202	0.4433	0.3049	**0.047**
θ_a 30 cm	0.07	0.00	−0.26	−0.11	0.05	0.38	1.00	0.07	−0.33	0.24	0.40
	0.2123	0.9346	**<0.0001**	0.0681	0.3713	**<0.0001**		0.2751	**<0.0001**	**<0.0001**	**<0.0001**
D_s/D_o 30 cm	0.02	−0.12	0.05	0.18	0.06	0.02	−0.33	0.12	1.00	0.27	0.48
	0.7615	**0.0352**	0.4433	**0.002**	0.3247	0.6854	**<0.0001**	**0.0416**		**<0.0001**	**<0.0001**
K_s 30 cm	0.12	−0.08	−0.12	0.02	0.01	0.26	0.40	0.21	0.48	0.56	1.00
	0.0476	0.1706	**0.047**	0.7787	0.8886	**<0.0001**	**<0.0001**	**0.0003**	**<0.0001**	**<0.0001**	

Note: The table introduces the correlation coefficient followed below by the associated probability. Probability in bold is significant at $p = 0.05$ and below. All abbreviations are detailed in the list.

relationship between air-filled porosity θ_a and crop yields is also surprising. However, the range of θ_a values (on average about 0.05 cm^3 cm^{-3}) is rather characteristic of severe aeration limitations, as highlighted above. Interestingly, θ_a was negatively correlated to relative gas diffusivity ($p = -0.33$, $p < 0.0001$) at the 30-cm depth. This may be somewhat unexpected as θ_a partly controls relative gas diffusivity and is commonly used in its calculation as D_s/D_o calculation is partly based on the water desorption curve (Caron & Nkongolo, 2004). However, consistent with this negative correlation, such a counterintuitive relationship has been observed for growing media. It was explained by the fact that θ_a alone is not an indicator of pore connectivity, as outlined by previous authors, while K_s, on the other hand, is influenced by pore connectivity and strongly affects the calculation of D_s/D_o (Caron & Nkongolo, 2004). Herein, the positive correlation between relative gas diffusivity and K_s at the 30 cm ($r = 0.48$, $p < 0.0001$) also supports the above explanation. The nonsignificant or negative correlation between D_s/D_o ($r = 0.05$, $p = 0.44$) and K_s ($r = -0.12$, $p = 0.047$) on one side with BD at a depth of 30 cm on the other side also supports the statement that pore connectivity is partially characterized by BD (Chamindu et al., 2019).

3.1.2 | Artificial intelligence investigations

Instead of using all 38 important variables, the LIME results helped in selecting the top 10 features to develop a new machine learning model. The model's accuracy was slightly better than the one using all inputs. LIME provided a framework to identify key contributing variables for the multi-site-year corn response. By relative importance, it is seen (Figure 2) that post emergence applied nitrogen came first and NAG, an enzyme which is a key player in transitioning concentrations of nitrogen, carbon, and ammonium to the soil came second. Indeed, the activity of NAG enzymes can serve as an indicator of microbial activity and nutrient cycling in soil ecosystems. High levels of NAG activity often indicate healthy soil with active microbial communities capable of breaking down organic matter and recycling nutrients. Conversely, low NAG activity may suggest soil degradation or nutrient limitations. Rainfall in July, at the time of the exponential growth of corn, came third followed by microbial respiration. Such results suggests that nitrogen, appropriate enzymatic activities, and respiration were key elements for productivity. CHU, θ_s, at a depth 15 cm, phosphorus, and potassium as well as D_s/D_o at a depth of 30 cm were among variables with a positive impact on the corn yield response. On the contrary, magnesium, CHU in August, K_s at a depth of 15 cm and precipitation in June and August were negatively related to corn yield response. Globally, the model had

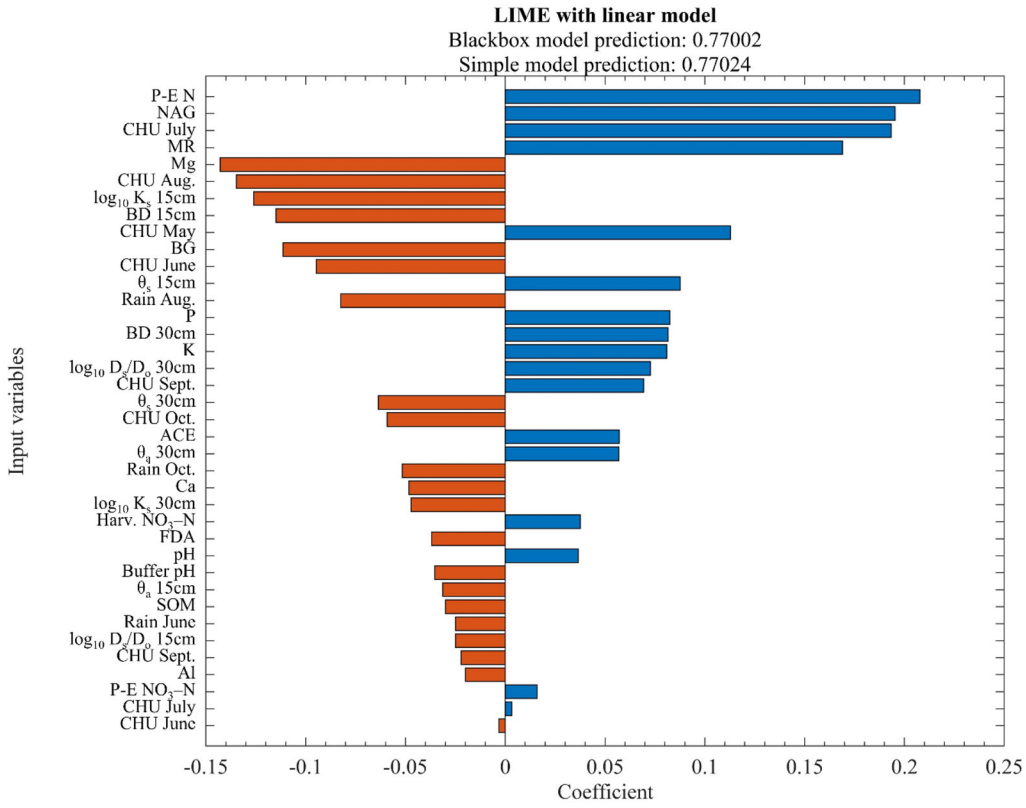

FIGURE 2 The impact of each feature on yield prediction using Local Interpretable Model-Agnostic Explanations (LIME). Positive effects are illustrated in blue and negative effects in red. All abbreviations are detailed in the list.

a correlation value of 0.85 (r^2 of 0.73) when using the first 10 variables. These trends are logical for nitrogen, given the fact that this was an N trial with all sites being tested with a wide range of applications (50–300 kg N ha^{-1}). Compaction issues were revealed through positive relationships for D_s/D_o and total porosity θ_s at 15 cm and a negative relationship with BD at 15 cm. On the contrary, the positive relationship between BD (at 30 cm) and crop yield and the negative relationship between θ_s (at 30 cm) and crop yield are rather counterintuitive. This may be linked to the fact that these parameters were negatively correlated with relative gas diffusivity (D_s/D_o) at that depth, as described above.

3.1.3 | Regression studies involving static and dynamic parameters

Stepwise multiple regression analyses were also performed for 18 sites using the same data set and same parameters: soil physical static and dynamic parameters, chemical parameters, biological parameters, and meteorological indicators (CHU and rainfall). Overall, the R^2 reached 0.70 and yielded similar results as those reported above with respect to most relevant variables/predictors (results not shown here). A dummy coding regression model, including a site, a year, and a site by year interaction term, was also performed to investigate whether unknown variables bound to the site (management, time of seeding, hybrid) which were not measured or available could help improve the prediction. In the end, a small improvement was achieved (R^2 at 0.73). Some key physical parameters remained (K_s at 15 cm and θ_s at 30 cm; data not shown). This suggests that the variability of crop response to environmental parameters, soil properties and measurements of variables, and nonlinearity of the response to some parameters contributed to the remaining unexplained proportion of the variance, that is about 0.27 (1-R^2).

As highlighted above, the three sites known to have compacted and uncompacted zones and that were all in corn production during the same year (2019) were kept to investigate the performance of soil health indicators (bulk density, air filled porosity at −5 kPa, saturated hydraulic conductivity, and relative gas diffusivity). For these three sites, air-filled porosity at −5 kPa varied from 0.02 to 0.25 cm^3 cm^{-3}, therefore allowing to run a regression analysis within the range of an expected positive crop response to increasing air-filled porosity (Table 4). Bulk density also varied from 1.09 to 1.76 g cm^{-3}, K_s varied from 4.79×10^{-5} to 0.33 cm s^{-1}, and D_s/D_o varied from 2.51×10^{-8} to 0.0251, covering the range

TABLE 4 Descriptive statistics of static and dynamic physical properties of the three sites sampled in 2019 showing compaction problems.

Variables	Depth (cm)	Units	No. of observations	Mean	Standard deviation	Minimum	Maximum
Post emergence nitrogen		kg ha^{-1}	41	109.76	77.64	0	250
BD	15	g cm^{-3}	41	1.46	0.15	1.10	1.71
BD	30	g cm^{-3}	41	1.52	0.15	1.16	1.76
θ_s	15	cm^3 cm^{-3}	41	0.43	0.06	0.34	0.57
θ_s	30	cm^3 cm^{-3}	41	0.42	0.06	0.32	0.55
θ_a	15	cm^3 cm^{-3}	41	0.11	0.05	0.02	0.25
θ_a	30	cm^3 cm^{-3}	41	0.11	0.06	0.03	0.24
K_s[a]	15	cm s^{-1}	41	8.12E-03	6.38	1.85E-04	6.93E-01
K_s[a]	30	cm s^{-1}	41	8.00E-03	8.58	4.99E-05	3.28E-01
D_s/D_o[a]	15	cm^2 s^{-1} cm^{-2} s^1	41	4.95E-04	11.5	9.05E-07	1.74E-02
D_s/D_o[a]	30	cm^2 s^{-1} cm^{-2} s^1	41	2.00E-04	52.5	2.50E-08	6.85E-02

Note: See table of abbreviations for descriptions. Values in the table are back transformed.

[a]Calculated on log transformed data.

TABLE 5 Stepwise regression parameters between static and dynamic indicators of Table 4 and corn dry yield response for the three sites selected with compaction problems in 2019.

Step	Effects	Adjusted R^2	F value	Prob> F	Estimated parameter	Standard error of estimate	T-value
0.00	Intercept	0.00	0.00	1.0000	7991.93	548.62	14.57
1.00	Applied N	0.42	29.42	<0.0001	12.63	2.39	5.29
2.00	Log10 D_s/D_0 30 cm	0.53	10.84	0.0022	354.49	107.68	3.29

of parameter values leading to deficient crop response due to poor drainage and aeration (Table 4). The year 2019 was a year with normal yields at 9.37 ha^{-1} against 9.96 tonnes ha^{-1} for the 2017–2022 period. A multivariate regression was performed using variables in Table 4 to test the sensitivity of soil health indicators to explain yield variability, while considering applied nitrogen and all physical parameters, in linear and quadratic forms.

Table 5 shows that two parameters (applied nitrogen and the log10 of D_s/D_o at a depth of 30 cm) could explain 53% (adjusted R^2) of the yield variability of the three sites. Estimated parameters were also consistent and positive, indicating that the higher the applied nitrogen and the higher the relative gas diffusivity, the higher the yields. This suggests that gas exchange properties represented a significant explanatory variable of grain corn yield throughout the three studied sites in addition to the corn response to nitrogen fertilization. No significant relationships for the static parameters (θ_a and BD) were observed. This conclusion is quite logical given the low levels of aeration observed, the latter promoting denitrification, affecting root respiration, and possibly crop response to its environment, nitrogen application and dynamic indicators.

3.2 | Evaluating potential compaction effects on corn N response

The sensitivity of the crop to aeration conditions at different nitrogen levels was investigated on other sites by further looking at crop response under different drainage conditions. In fall 2021 and spring of 2022, drainage conditions were characterized from water table observations depicted by the piezometer network installed perpendicular to the drainage network (Figure 3).

For the five sites, water table variation in early spring indicated that site 5 had a uniform and fast drainage with a K_s 5.37 $\times$ 10^{-4} cm s^{-1} at the 30-cm depth and an intermediate D_s/D_o of 1.18 $\times$ 10^{-3} (values in legend of Figure 4). Sites 8 and 9 had non-uniform drainage with some locations with a high-water table despite a high K_s at 30 cm. This suggests a problematic drainage system (plugged drains, a low K_s value below 40 cm, deeper compaction issues, uneven drains, damaged drains, etc.). Sites 7 and 14 drained slowly, with a high-water table around one of the piezometers in site 7. The latter two sites had low K_s at the 30-cm depth (9.57 $\times$ 10^{-6} cm s^{-1} and 3.85 $\times$ 10^{-5} cm s^{-1}, Figure 4). The top crop yield site (site 5) had more uniform drainage than the others, with the water table drawing down uniformly to about 80–100 cm early

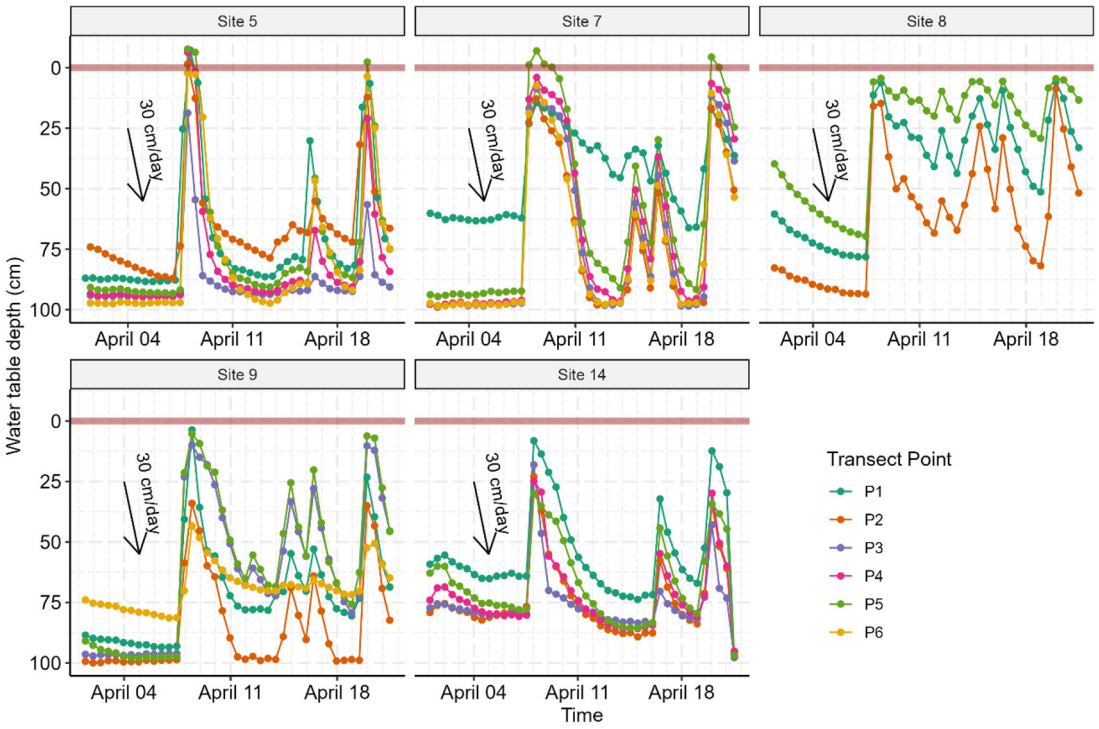

FIGURE 3 Water potential measured in six piezometers of five sites randomly chosen for spring 2022. The piezometers were installed on a transect perpendicular to the main subsurface drain direction. The total distance of the installation covered the full distance between two adjacent corrugated drains and piezometers were equally spaced in between. Some piezometers data were removed due to malfunctioning or data losses.

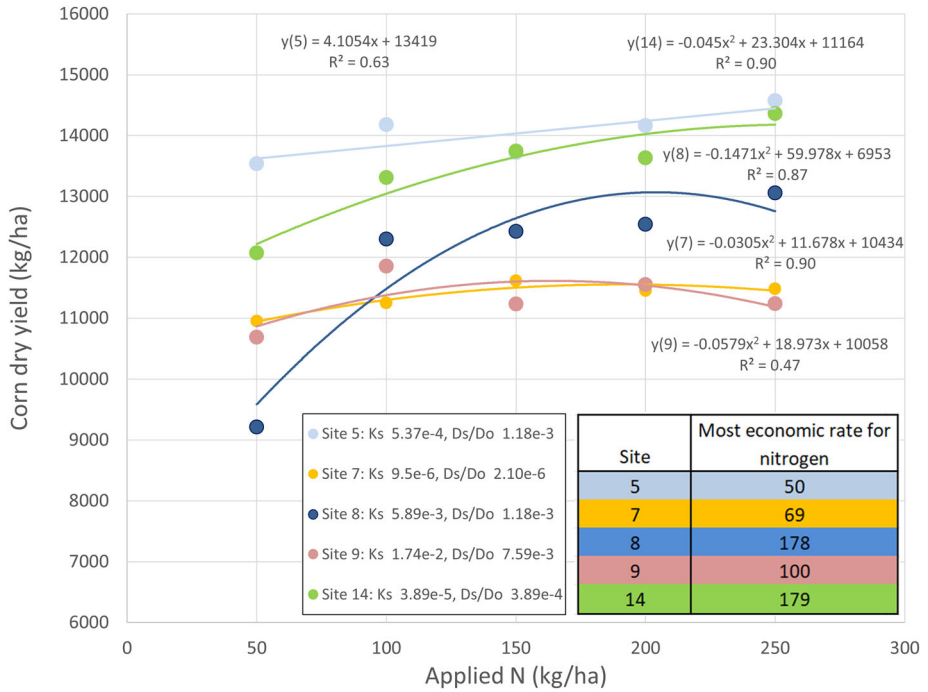

FIGURE 4 The relationship between corn dry yield and nitrogen for five sites randomly chosen and monitoring piezometers in 2022. Polynomial regression equations are given for each site (e.g., Site 5: y(5)) and were used to calculate the most economic rate for nitrogen or the rate of nitrogen (N) fertilizer that provides the greatest economic return (Equations 4 and 5). This is important economically, but also environmentally as most economic rate for nitrogen (MERN) represents an N rate that meets crop requirements without excess, avoiding environmental costs of producing excess fertilizer or leaving excess N in the environment.

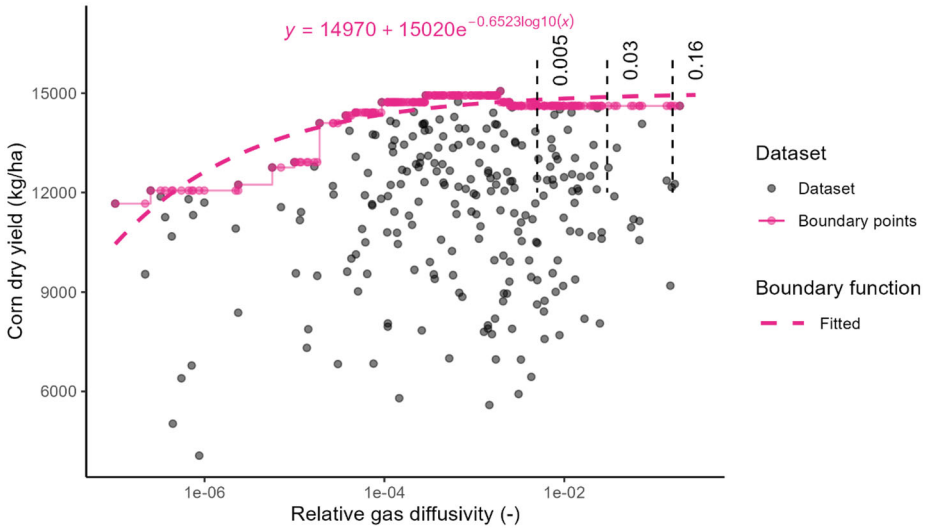

FIGURE 5 Relationship between the relative gas diffusivity at the 30-cm depth and corn dry yields for the whole data set.

in spring and observed water table positions within drainage norms.

In the presence of aeration and drainage limitations in compacted sites, denitrification is expected to affect the crop response to fertilization. Figure 4 presents the relationship between applied nitrogen and corn yield for the five sites with installed piezometer in 2021. We can see that site 5, with a K_s appropriate (5.37×10^{-4} cm s^{-1}) and an intermediate D_s/D_o (1.18×10^{-3}) had the most even water table and showed the highest yields and required the lowest nitrogen at the maximum economic yield (50 kg ha^{-1}). Site 14 had a slow drainage, with the second lowest K_s and the second lowest D_s/D_o, and required the maximum N application (179 kg ha^{-1}) to reach the maximum economical yield. Site 7, with the lowest K_s and D_s/D_o, had the lowest yield and a very poor response to nitrogen, possibly caused by a zone with a high-water table limiting crop growth and denitrification losses. Site 9, despite optimal properties of the top layer (highest K_s and D_s/D_o at 30 cm), showed a small response to nitrogen (MERN at 100 kg ha^{-1}) but may still have drainage problem as suggested by a non-uniform water table depth on this site (Figure 3). Finally, site 8 with intermediate K_s and D_s/D_o at 30 cm required high nitrogen input (178 kg ha^{-1}) to get the maximum yield, possibly due also to its non-uniform water table, the one site with the closest to the surface water table among the five sites. The absence of response or high requirements to reach maximum economical yield in soils with high and uneven water tables and low relative gas diffusivity suggests that a high proportion of applied nitrogen may be respired by microbes or leached out, with too poorly developed root systems for optimal uptake. Interestingly, the top crop yield site (site 5) had an optimum economic rate of 50 kg N per hectare, suggesting naturally good growing conditions despite relatively low nitrogen application. Early rapid growth with efficient N uptake could also be a possible explanation for such good performances. The two sites with lower yields and a weak response to nitrogen fertilization had the maximum economic yield being achieved at about 75 kg per hectare (100 and 69 for sites 9 and 7), a rate lower than what a lot of producers usually apply (150–200 kg ha^{-1}). Also of interest is the difference in optimal rate between the top crop yield site 5 (50) and intermediate yield ones (178 and 179) in terms of optimal nitrogen requirement. A difference of about 50–70 kg ha^{-1} is often observed in long-term rotation studies and could be due to several soil health factors and organic nitrogen mineralization rates observed between sites (Drury et al., 2014; Giroux et al., 2008). We observed larger differences between optimal rates between sites, at about 120 kg ha^{-1}, suggesting an important loss of nitrogen efficiency.

Another way of analyzing the data when facing a complex response to soil parameters, weather data, and unknown additional factors is to use a boundary line approach with large data sets (Schnug et al., 1996; Webb, 1972). Such approach assumes that when all other factors are nonlimiting, the upper *Y*-axis asymptote of the yield-factor (herein diffusivity) regression plot will help in identifying the zone of sufficient diffusivity for maximum yield. Figure 5 introduces the corn dry yield for the whole data set with respect to the relative gas diffusivity. Boundary lines were drawn using all boundary data and a plateau model fitted to those data. It is seen that the exponential plateau predicts maximum yield at the highest D_s/D_o value (0.16). This is usually, the maximum value that most soils can reach for D_s/D_o (Chamindu et al., 2019). This suggests aeration-limiting conditions in early spring for most soils studied, then consistent with extensive compaction and lack of aeration observed in most soils. With this model though, it is difficult to identify a clear threshold for gas diffusivity limitation, an important yield

drop being observed at D_s/D_o value below 0.0001. It should be mentioned that while consistent with the physical role of gas exchange on crop response, the estimates of D_s/D_o remain approximative as the methodology used for the calculations may present biases (Caron & Nkongolo, 2004). Additional studies are therefore required for better accuracy of relative gas diffusivity critical values for corn under field conditions, but this study points out the relevance of using such an index to assess soil health quality, as well as hydraulic conductivity as seen above.

3.2.1 | Practical implications

With respect to land degradation, this study suggests that dynamic indicators should be used in addition to static parameters for a more complete assessment of soil health, as already reported in previous studies. These results also suggest that an assessment of key soil physical indicators could potentially guide nitrogen application recommendation to limit the risk of denitrification and optimize N use.

3.2.2 | Future work

With respect to the use of indicators, future work should look at dynamic indicators in addition to static indicators to diagnose compaction limitations of additional sites and extend to deeper soil layers. The extent of compaction increase should be checked as soil health indicators do not specifically include such assessment systematically and the compaction problem is expected to increase further (Keller & Or, 2022). Additional work is needed in other corn-producing areas to have a more complete diagnosis of land degradation associated with long-term corn production and nitrous oxide emission. Indeed, gas diffusivity is related to denitrification fluxes and to the risk of denitrification (Nkongolo et al., 2010) and to evaluate the effects on productivity and environmental outcomes (Hu et al., 2021). Future work should also investigate to which extent long-term forage rotation or agroforestry systems could restore or maintain the first soil layers and deeper horizons soil physical health conditions and compare the long-term economic viability of continuous row crop production with such systems.

AUTHOR CONTRIBUTIONS

Jean Caron: Conceptualization; funding acquisition; methodology; project administration; resources; supervision; writing—original draft; writing—review and editing. **Vincent Grégoire**: Investigation; methodology; resources; software; writing—original draft; writing—review and editing. **Alain Rousseau**: Conceptualization; funding acquisition; methodology; writing—original draft. **Jacynthe Dessureault-Rompré**: Funding acquisition; methodology; resources; writing—original draft; writing—review and editing. **Gabriel Deslauriers**: Formal analysis; methodology; resources; writing—original draft. **Diane Bulot**: Data curation; formal analysis; investigation; methodology; resources; software; supervision. **Josselin Bontemps**: Methodology; resources; writing—original draft. **Didier Vieux**: Investigation; methodology; resources; validation. **Thiago Gumiere**: Funding acquisition; methodology; writing—original draft. **Hossein Bonakdari**: Data curation; formal analysis; investigation; methodology; resources; validation; writing—original draft.

ACKNOWLEDGMENTS

The authors would like to thank Soleno Inc., Axelys, Elmec Inc., Groupe Pleine Terre, the Quebec Research Network for Sustainable Agriculture (www.rqrad.com), and the Natural Sciences and Engineering Research Council of Canada (NSREC) for financial support of the project.

CONFLICT OF INTEREST STATEMENT

The authors declare no conflicts of interest.

ORCID

Jean Caron https://orcid.org/0000-0003-4681-2373
Vincent Grégoire https://orcid.org/0000-0003-1491-8173
Jacynthe Dessureault Rompre https://orcid.org/0000-0002-2812-0691

REFERENCES

Adam, G., & Duncan, H. (2001). Development of a sensitive and rapid method for the measurement of total microbial activity using fluorescein diacetate (FDA) in a range of soils. *Soil Biology and Biochemistry*, *33*, 943–951.

Allaire, S. E., Caron, J., Duchesne, I., Parent, L. É., & Rioux, J. A. (1996). Air-filled porosity, gas relative diffusivity, and tortuosity: Indices of Prunus × cistena sp. growth in peat substrates. *Journal of the American Society for Horticultural Science*, *121*(2), 236–242.

Angers, D. A., & Caron, J. (1998). Plant-induced changes in soil structure: Processes and feedbacks. *Biogeochemistry*, *42*, 55–72.

Audet, R., Côté, H., Bachand, D., & Mailhot, A. (2012). *Atlas agroclimatique du Québec. Évaluation des opportunités et des risques agroclimatiques dans un climat en évolution*. https://numerique.banq.qc.ca/patrimoine/details/52327/2411887?docref=RR3mVyxl1hAeW3RpXp9gnA

Balaine, N. (2012). *Influence of soil bulk density and matric potential on relative gas diffusivity and urea/nitrate-derived N_2O and N_2 losses* [Doctoral dissertation, Lincoln University].

Balaine, N., Clough, T. J., Beare, M. H., Thomas, S. M., & Meenken, E. D. (2016). Soil gas diffusivity controls N_2O and N_2 emissions and their ratio. *Soil Science Society of America Journal*, *80*, 529–540. https://doi.org/10.2136/sssaj2015.09.0350

Balaine, N., Clough, T. J., Beare, M. H., Thomas, S. M., Meenken, E. D., & Ross, J. G. (2013). Changes in relative gas diffusivity explain soil

nitrous oxide flux dynamics. *Soil Science Society of America Journal*, *77*, 1496–1505. https://doi.org/10.2136/sssaj2013.04.0141

Ball, B. C. (2013). Soil structure and greenhouse gas emissions: A synthesis of 20 years of experimentation. *European Journal of Soil Science*, *64*, 357–373.

Ball, B. C., O'sullivan, M. F., & Hunter, R. (1988). Gas diffusion, fluid flow and derived pore continuity indices in relation to vehicle traffic and tillage. *Journal of Soil Science*, *39*, 327–339.

Batey, T. (2009). Soil compaction and soil management—A review. *Soil Use and Management*, *25*, 335–345.

Bell, C. W., Fricks, B. E., Rocca, J. D., Steinweg, J. M., McMahon, S. K., & Wallenstein, M. D. (2013). High-throughput fluorometric measurement of potential soil extracellular enzyme activities. *Journal of Visualized Experiments*, *81*, e50961.

Ben-Noah, I., & Friedman, S. P. (2018). Review and evaluation of root respiration and of natural and agricultural processes of soil aeration. *Vadose Zone Journal*, *17*, 1–47. https://doi.org/10.2136/vzj2017.06.0119

Boudreault, S., Pepin, S., Caron, J., Lamhamedi, M. S., & Paiement, I. (2014). Substrate aeration properties and growth of containerized white spruce: A case study. *Vadose Zone Journal*, *13*(3), 1–15. https://doi.org/10.2136/vzj2013.05.0081

Bourgeois, G., Audet, R., Bélanger, L., Duchesne, I., Filion, P., Leclerc, B., & Tremblay, G. (2012). *Mise à jour des unités thermiques maïs (UTM) au Québec*. Colloque en agroclimatologie. Centre de référence en agriculture et agroalimentaire du Québec, https://www.craaq.qc.ca/documents/files/Publications/EAGR1201_Cahier_participant.pdf (in French)

Caron, J. (2004). Defining new aeration and capillary rise criteria to assess the quality of growing media. In J. Päivänen (Ed.), *Proceedings of the 12th international peat congress* (pp. 221–228). International Peat Society.

Caron, J., & Nkongolo, N. V. (2004). Assessing gas diffusion coefficients in growing media from in situ water flow and storage measurements. *Vadose Zone Journal*, *3*, 300–311. https://doi.org/10.2136/vzj2004.3000

Caron, J., Pepin, S., & Periard, Y. (2013). Physics of growing media in a green future. *Acta Horticulturae*, *1034*, 309–317.

Caron, J., Price, J. S., & Rochefort, L. (2015). Physical properties of organic soil: Adapting mineral soil concepts to horticultural growing media and histosol characterization. *Vadose Zone Journal*, *14*, 1–14. https://doi.org/10.2136/vzj2014.10.0146

Caron, J., Banton, O., Angers, D. A., & Villeneuve, J. P. (1996). Preferential bromide transport through a clay loam under alfalfa and corn. *Geoderma*, *69*, 175–191.

Caron, J., Elrick, D. E., Beeson, R., & Boudreau, J. (2005). Defining critical capillary rise properties for growing media in nurseries. *Soil Science Society of America Journal*, *69*, 794–806. https://doi.org/10.2136/sssaj2004.0108

Caron, J., Schmilewski, G., Alsanius, B. W., Zheng, Y., & Michel, J. C. (2022). An updated glossary of terms and basic characteristics of growing media. *Acta Horticulturae*, *1377*, 925–934.

CEAEQ. (2014). Détermination des métaux assimilables et du phosphore : méthode par spectrométrie de masse à source ionisante au plasma d'argon, MA. 200 – Mét-P ass. 1.0, Rév. 2. Ministère du Développement durable, de l'Environnement et de la Lutte contre les changements climatiques du Québec.

Chabot, R., Caron, J., Garon, B., Guillou, M., Julien, R., Laberge, D., Lagacé, R., Ménard, O., Petit, V., & Savoie, V. (2022). *Guide Diagnostic et drainage souterrain des terres agricoles*. (*Diagnosis guide for subsurface drainage of agricultural fields*). CRAAQ. (in French).

Chamindu, D. T., Clough, T. J., Thomas, S. M., Balaine, N., & Elberling, B. (2019). Density effects on soil-water characteristics, soil-gas diffusivity, and emissions of N_2O and N_2 from a re-packed pasture soil. *Soil Science Society of America Journal*, *83*, 118–125. https://doi.org/10.2136/sssaj2018.01.0048

CPVQ—Conseil des productions végétales du Québec. (1993). *Mise à jour des Méthodes d'analyse des sols, des fumiers et des tissus végétaux. Commission des sols, section méthodologie*. Québec (Canada). AGDEX 533.

Daddow, R. L., & Warrington, G. E. (1983). *Growth-limiting soil bulk densities as influenced by soil texture* (WSDG report WSDG-TN-00005). Watershed Systems Development Group USDA Forest Service.

Drury, C. F., Reynolds, W. D., Tan, C. S., McLaughlin, N. B., Yang, X. M., Calder, W., Oloya, T. O., & Yang, J. Y. (2014). Impacts of 49–51 years of fertilization and crop rotation on growing season nitrous oxide emissions, nitrogen uptake and corn yields. *Canadian Journal of Soil Science*, *94*, 421–433.

Gameda, S., Raghavan, G. S. V., McKyes, E., & Thériault, R. (1987). Subsoil compaction in a clay soil. I. Cumulative effects. *Soil and Tillage Research*, *10*, 113–122.

Gasser, M.-O., Bossé, C., Clément, C. C., Bernard, C., Grenon, L., Mathieu, J.-B., & Tremblay, B. M. E. (2023). *Report one on agricultural land soil health in Québec: study of the main soil series*(Report). Ministère de l'Agriculture, des Pêcheries et de l'Alimentation (MAPAQ). (in French).

Giroux, M., N'Dayegamiye, A., & Lemieux, M. (2008). *Rear effects of mineral and organic fertilizer application and rotation on crop yield and nitrogen in requirements of corn*. Cahiers de l'observatoire des sols du Québec. (in French).

Gliński, J., & Stępniewski, W. (2018). *Soil aeration and its role for plants*. CRC Press.

Håkansson, I., Voorhees, W. B., Elonen, P., Raghavan, G. S. V., Lowery, B., Van Wijk, A. L. M., Rasmussen, K., & Riley, H. (1987). Effect of high axle-load traffic on subsoil compaction and crop yield in humid regions with annual freezing. *Soil and Tillage Research*, *10*, 259–268.

Haney, R., Brinton, W., & Evans, E. (2008). Soil CO_2 respiration: Comparison of chemical titration, CO_2 IRGA analysis and the Solvita gel system. *Renewable Agriculture and Food Systems*, *23*, 171–176.

Hu, W., Drewry, J., Beare, M., Eger, A., & Müller, K. (2021). Compaction induced soil structural degradation affects productivity and environmental outcomes: A review and New Zealand case study. *Geoderma*, *395*, 115035.

Hurisso, T. T., Moebius-Clune, D. J., Culman, S. W., Moebius-Clune, B. N., Thies, J. E., & Van Es, H. M. (2018). Soil protein as a rapid soil health indicator of potentially available organic nitrogen. *Agricultural & Environmental Letters*, *3*(1), 180006. https://doi.org/10.2134/ael2018.02.0006

Keller, T., & Or, D. (2022). Farm vehicles approaching weights of sauropods exceed safe mechanical limits for soil functioning. *Proceedings of the National Academy of Sciences*, *119*(21), e2117699119.

Lepage, M.-P. B., & Bélanger, G. (2012). *Indices agrométéorologiques pour l'aide à la décision dans un contexte de climat variable et en évolution*. Centre de référence en agriculture et agroalimentaire du Québec (CRAAQ). https://agrometeo.solutions-mesonet.org/help/feuillet_CRAAQ_indices_agrometeo.pdf (in French)

Meek, B. D., DeTar, W. R., Rechel, E. R., Carter, L. M., & Rolph, D. (1990). Infiltration rate as affected by an alfalfa and no-till cotton cropping system. *Soil Science Society of America Journal*, *54*, 505–508.

Mehrabi, Z. (2023). Likely decline in the number of farms globally by the middle of the century. *Nature Sustainability*, *6*, 949–954.

Moore, T. (2021). Soils of Quebec. In *Digging into Canadian soils*. Canadian Society of Soil Science. https://openpress.usask.ca/soilscience/chapter/soils-of-quebec/

Nemati, M. R., Caron, J., Banton, O., & Tardif, P. (2002). Determining air entry value in peat substrates. *Soil Science Society of America Journal*, *66*(2), 367–373. https://doi.org/10.2136/sssaj2002.3670

Nkongolo, N. V., Hatano, R., & Kakembo, V. (2010). Diffusivity models and greenhouse gases fluxes from a forest, pasture, grassland and corn field in Northern Hokkaido Japan. *Pedosphere*, *20*, 747–760.

Piccoli, I., Schjønning, P., Lamandé, M., Zanini, F., & Morari, F. (2019). Coupling gas transport measurements and X-ray tomography scans for multiscale analysis in silty soils. *Geoderma*, *338*, 576–584.

R Core Team. (2023). *R: A language and environment for statistical computing*. R Foundation for Statistical Computing. https://www.R-project.org/

Reynolds, W. D. (2008). Saturated hydraulic properties: Laboratory methods. In M. R. Carter & E. G. Gregorich (Eds.), *Soil sampling and methods of analysis* (pp. 1013–1024). Canadian Society of Soil Science.

Reynolds, W. D., Drury, C. F., Yang, X. M., Tan, C. S., & Yang, J. Y. (2014). Impacts of 48 years of consistent cropping, fertilization and land management on the physical quality of a clay loam soil. *Canadian Journal of Soil Science*, *94*, 403–419.

Reynolds, W. D., & Topp, G. C. (2008). Soil water desorption and imbibition: Tension and pressure techniques. In M. R. Carter & E. G. Gregorich (Eds.), *Soil sampling and methods of analysis* (pp. 981–997). Canadian Society of Soil Science.

Rosser, B. (2022). Understanding MERN (most economic rate of nitrogen) for corn. *Field Crop News*. https://fieldcropnews.com/2022/04/understanding-mern-most-economic-rate-of-nitrogen-for-corn/

Schnug, E., Heym, J., & Achwan, F. (1996). Establishing critical values for soil and plant analysis by means of the boundary line development system (bolides). *Communications in Soil Science and Plant Analysis*, *27*, 2739–2748. https://doi.org/10.1080/00103629609369736

Stepniewski, W., Gliński, J., & Ball, B. C. (1994). Effects of compaction on soil aeration properties. In *Developments in agricultural engineering* (Vol. 11, pp. 167–189). Elsevier.

Tabi, M., Tardif, L., Carrier, P., Laflamme, G., & Rompré, M. (1990). *Inventaire des problèmes de dégradation des sols agricoles du Québec* (Publication No. 90—130156). Rapport Synthèse. Ministère de l'Agriculture, des Pêcheries et de l'Alimentation du Québec.

Thériault, L., Dessureault-Rompré, J., & Caron, J. (2019). Short-term improvement in soil physical properties of cultivated histosols through deep-rooted crop rotation and subsoiling. *Agronomy Journal*, *111*, 2084–2096. https://doi.org/10.2134/agronj2018.04.0281

van Genuchten, M. Th. (1980). A closed-form equation for predicting the hydraulic conductivity of unsaturated soils. *Soil Science Society of America Journal*, *44*, 892–898. https://doi.org/10.2136/sssaj1980.03615995004400050002x

Webb, R. A. (1972). Use of the boundary line in the analysis of biological data. *Journal of Horticultural Science*, *47*, 309–319.

Xu, X., Nieber, J. L., & Gupta, S. C. (1992). Compaction effect on the gas diffusion coefficient in soils. *Soil Science Society of America Journal*, *56*, 1743–1750. https://doi.org/10.2136/sssaj1992.03615995005600060014x

Yi, J., Hu, W., Beare, M., Liu, J., Cichota, R., Teixeira, E., & Guo, L. (2022). Treading compaction during winter grazing can increase subsequent nitrate leaching by enhancing drainage. *Soil and Tillage Research*, *221*, 105424.

Ziadi, N., & Tran, T. S. (2008). Mehlich 3-extractable elements. In M. R. Carter & E. G. Gregorich (Eds.), *Soil sampling and methods of analysis* (pp. 81–88). Canadian Society of Soil Science.

How to cite this article: Caron, J., Grégoire, V., Rousseau, A. N., Rompre, J. D., Deslauriers, G., Bulot, D., Bontemps, J., Vieux, D., Gumiere, T., & Bonakdari, H. (2025). Using relative gas diffusivity to highlight soil compaction issues with possible effects on N efficiency in grain corn production, southern Quebec, Canada. *Vadose Zone Journal*, *24*, e70019. https://doi.org/10.1002/vzj2.70019